

## Intrinsic linewidths of image-potential states on Ni(111)

N. Fischer, S. Schuppler, Th. Fauster, and W. Steinmann

*Sektion Physik, Universität München, Schellingstrasse 4, D-8000 München 40, Federal Republic of Germany*

(Received 16 July 1990)

With high-resolution two-photon photoemission we fully resolved the lowest three image-potential states on Ni(111) and measured the intrinsic linewidths of the two lowest states. The values  $84 \pm 10$  and  $12 \pm 10$  meV are substantially larger than experimental results and theoretical predictions for other surfaces. A decrease in linewidth of the lowest state after adsorption is observed and indicates that surface states are involved in the decay mechanism. Further possible reasons for this large intrinsic linewidth on Ni(111) are discussed.

An electron in front of a metal surface feels the attractive force of its own image charge. If the electron reflectivity of the metal surface is high, especially if a relative band gap of available bulk states exists, the electron is trapped in the potential well between the surface and the Coulombic image potential. This leads to a Rydberg-like series of states converging towards the vacuum level—the image-potential states. The wave functions of these states are localized almost completely outside the metal and therefore only weakly coupled to the bulk. Thus image-potential states have substantially longer lifetimes than bulk states with comparable energy. As the overlap between wave functions of image states and bulk states decreases with the order  $n$  of the state, an increase of the lifetime for higher image states is expected. Theory finds an  $n^3$  power law.<sup>1,2</sup> Early measurements of image states by two-photon photoemission spectroscopy (2PPES) could resolve the first two members of the series.<sup>3</sup> The accuracy of the measured binding energies and dispersions was good enough to distinguish between different theoretical models for image-potential states. Excellent agreement with the predictions of the phase analysis model<sup>4</sup> has been found for a number of materials and faces.<sup>3,5</sup>

The measurement process for 2PPE is depicted in Fig. 1(a). Pulsed laser light is used to excite electrons from occupied states below the Fermi energy  $E_F$  into unoccupied states below the vacuum level  $E_V$ . Within the lifetime of the excited state a second photon may be absorbed and photoemission from the intermediate state can be observed. In Figs. 1(b) and 1(c) possible decay channels for image-potential states are sketched. The lifetime of the  $n=1$  state might be determined by decay into empty bulk states via electron-hole pair production [Fig. 1(b)]. The two surface states  $S_0$  and  $S_1$  (Ref. 6) which have large overlap with image states may be involved in this process. For the higher members of the series radiative transition into lower states can play a significant role [Fig. 1(c)].<sup>7</sup> The scattering by defects and phonons might further decrease the lifetime of electrons in image-potential states.<sup>8</sup>

In recent years theoretical work has been done on the lifetime of image-potential states.<sup>2,7,9</sup> There the decay of the  $n=1$  state into empty bulk states via electron-hole pair production is considered [Fig. 1(b)] and yields an intrinsic linewidth of  $\Gamma(1) \approx 10$  meV for fcc (100) surfaces.<sup>9</sup> For Cu(111) the vacuum level lies closer to the

upper band-gap edge resulting in stronger penetration of the image-state wave function into the metal. So an increased lifetime broadening of about 20 meV is expected. The width of the  $n=2$  state—if it lies in the band gap—is determined by the radiative transition into the  $n=1$  state [Fig. 1(c)] and amounts to  $\Gamma(2) \approx 1$  meV.<sup>7</sup>

Experimental data for the lifetime of image states exist only for Ag(100). In a time-resolved 2PPE experiment using laser pulses with a duration in the range of 55–90 fs Schoenlein *et al.* measured lifetimes for the first two states of 15–35 and  $180 \pm 20$  fs, respectively.<sup>10</sup> Using  $\tau\Gamma = \hbar$  this gives widths of 19–44 and  $3.7 \pm 0.4$  meV, respectively. Nielsen, Brostroem, and Matthias found, in conventional 2PPES with an analyzer resolution of 70 meV, a width of  $35 \pm 9$  meV for the first state.<sup>11</sup> In a recent bichromatic 2PPE measurement with significantly better resolution of  $\approx 25$  meV we determined the widths of the first two states to be  $21 \pm 4$  and  $5 \pm 5$  meV.<sup>12</sup> So the experimental values are in fair agreement with theory.

Details of the experimental setup have been published previously.<sup>3</sup> A frequency-doubled tunable dye laser pumped by an excimer laser is used as the light source for

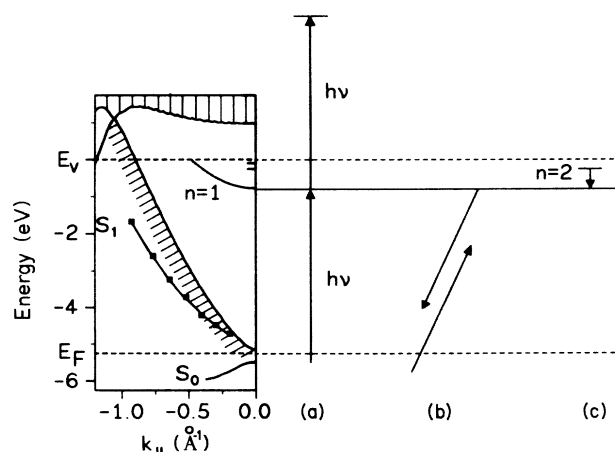


FIG. 1. Band structure for Ni(111) with image-potential states in the projected bulk band gap and two surface states  $S_0$  and  $S_1$  (from Ref. 6). (a) Two-photon photoemission via the first image state. Decay of image states: (b) via electron-hole pair creation and (c) radiative transition of the  $n=2$  state into the  $n=1$  state.

2PPE. To avoid space-charge effects we restricted the light intensity to less than  $1 \text{ mJ/cm}^2$ . The photoelectrons are analyzed in a sectoral hemispherical analyzer with an angular resolution better than  $\pm 2^\circ$  and capable of an energy resolution of around  $25 \text{ meV}$ . We used the procedure described in Ref. 12 to determine the energy resolution of the analyzer at the low-energy cutoff of photoemission spectra. The experiments have been carried out under UHV conditions ( $p \approx 5 \times 10^{-11} \text{ Torr}$ ). Auger electron spectroscopy, low-energy electron diffraction (LEED), one-photon photoemission, and 2PPE was used to check the surface cleanliness and quality. Sharp LEED spots on a low background were the result of a careful sample preparation.

The experimental resolution achieved in our experiment is demonstrated in the two 2PPE spectra shown in Fig. 2. Both spectra were recorded in normal emission at an analyzer pass energy of  $1.3 \text{ eV}$  but at different photon energies of  $5.210$  and  $5.102 \text{ eV}$ . In the upper spectrum we succeeded in fully resolving the first three image-potential states. Since the photon energy in this spectrum lies close to the work function of Ni(111), which we determined to  $5.25 \text{ eV}$ , the onset of the direct photoemission produces a shift and a broadening of the peaks due to space-charge effects. The peak separations, however, remain unchanged<sup>5</sup> and can be referred to the binding energy of the first state measured at lower photon energies where no space-charge effects are observed. In spite of the addi-

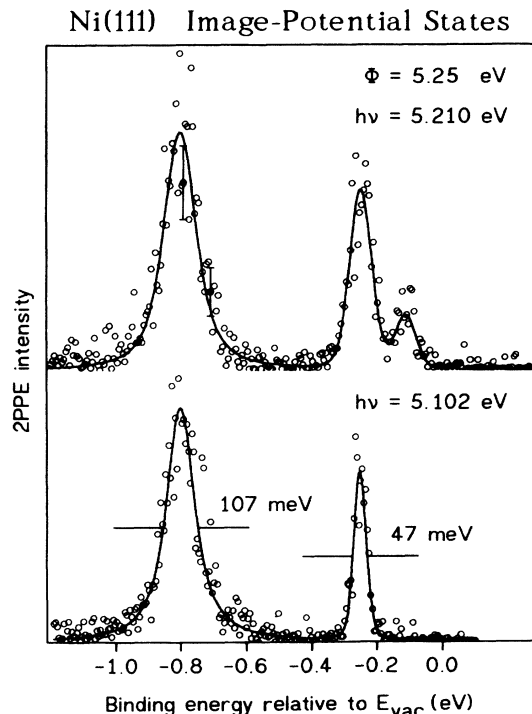


FIG. 2. 2PPE spectra for different photon energies. The solid line is the best fit of a model function to the data points (see text). Upper panel: The first three image-potential states excited with a photon energy close to the work function  $\Phi$ . Lower panel: The lower photon energy avoids space-charge effects and gives smaller overall peak widths. This photon energy is too low to excite the third image state.

tional space-charge broadening a decrease in linewidth from the lowest state to the higher ones can be clearly seen. To avoid these space-charge problems we chose lower photon energies for the linewidth measurement. The lower spectrum in Fig. 2 shows an extremely narrow linewidth for the  $n=2$  with a full width at half maximum (FWHM) of  $47 \text{ meV}$ . The solid line is the  $\chi^2$  fit of a model function to the data points. Assuming a Lorentzian intrinsic line shape we obtained the model function by a convolution with a Gaussian accounting for the analyzer resolution. The fitting parameters are the binding energies of the Lorentzians, their amplitudes and widths, and the width of the Gaussian. In order to rule out possible influences of sample preparation or analyzer resolution on the determined intrinsic linewidths we measured 15 spectra with the analyzer resolution set to three different values. We obtained consistent fits with intrinsic linewidths (FWHM) of  $84 \pm 10 \text{ meV}$  for the  $n=1$  state and  $12 \pm 10 \text{ meV}$  for the  $n=2$  state. We point out that the FWHM of the  $n=2$  state as it appears in the spectrum is a strict upper limit for the analyzer resolution in the fit. Consequently, fitting both states simultaneously leads to a significantly increased reliability of the fit. Additional broadening effects with non-Lorentzian distributions like remaining space-charge effects would lead to contributions in the Gaussian width and are indeed observed. For all spectra the Gaussians determined from the two-peak spectra were slightly broader ( $< 20\%$ ) than those determined at the respective low-energy cutoffs which are measured with significantly lower light intensities. This effect, however, does not influence the results for the intrinsic width, which can clearly be seen from the fact that the Lorentzian width of the  $n=1$  state in the upper, strongly broadened spectrum is  $80 \text{ meV}$  and so within the error limits. In contrast to that, the Gaussian widths (FWHM) are  $72$  and  $40 \text{ meV}$  for the upper and lower spectrum, respectively. In agreement with our recent work<sup>5</sup> we determined the difference in binding energies between the first and the second and the second and the third state to be  $547 \pm 6$  and  $136 \pm 25 \text{ meV}$ , respectively.

Calculations for Ni(111) do not yet exist. Following the present calculation for Cu(111),<sup>7</sup> one can estimate the trend for Ni(111): For this face the energy difference between the vacuum level and the upper edge of the band gap at  $k_{\parallel}=0$  is larger than on Cu(111), resulting in a smaller penetration of the image-state wave function into the bulk. Therefore one would expect an even smaller linewidth than the calculated value of  $20 \text{ meV}$  for Cu(111). But in contrast to that the width of the lowest image-potential state on Ni(111) is at least four times larger than this value.

We do not think that this discrepancy results from residual defects on the surface since special care was taken in preparing the sample. Additional support for this view comes from the following experiment: After exposure of the sample to the residual gas (mainly hydrogen) for  $1 \text{ h}$  a slight decrease ( $\approx 20\%$ ) in linewidth of the  $n=1$  state accompanied with a peak shift of  $27 \text{ meV}$  is observed. These changes are reversible by thermal desorption of the contamination. This decrease in linewidth is in contrast to

our studies on Ag(100) where an increase in linewidth of the first two image states upon oxygen adsorption was observed.<sup>12</sup>

One possible explanation for the large linewidth would be the magnetic properties of nickel. The one-step model of photoemission predicts an exchange splitting of 27 meV,<sup>13</sup> mainly due to the different band gaps for minority and majority spin electrons. We have tried fitting the  $n=1$  peak with two states of equal intensity and width and obtain significantly worse fits for splittings above 40 meV. The intrinsic linewidth, however, stays always within the error limits determined above. This is consistent with the observation that no change in linewidth occurs upon heating the sample above the Curie temperature. A significant contribution due to scattering by phonons can thus be excluded, too.

A further possible explanation is the high density of states near  $E_F$  for nickel as compared to copper. This is due to the fact that the flat  $d$  bands on nickel cross  $E_F$  whereas on copper they lie 2 eV lower. So an increase for the possibility of electron-hole pair production resulting in an increased linewidth can be expected.

The above-mentioned decrease in linewidth upon hydrogen adsorption indicates that an important contribution to the decay of image states on Ni(111) results from surface states. From the well-known fact that surface states on Ni(111) are very sensitive to contamination<sup>14</sup> we conclude

that the quenched surface states—that means quenched decay channels—are responsible for the decrease in linewidth. This is understandable since these states have larger overlap with the image states than bulk states. In the special case of Ni(111) there are two surface states near the Fermi level. Away from  $k_{\parallel}=0$ , the one crosses  $E_F$  and becomes unoccupied,<sup>6</sup> while the other disperses downwards and stays occupied (see Fig. 1). Since electron-hole pair production is not restricted in  $k_{\parallel}$  decay into empty surface states via electron-hole pair production including surface states might be a very efficient decay mechanism for image-potential states.

We conclude that calculations for the linewidth of image-potential states on Ni(111) seem highly desirable. The recent improvement of resolution and sensitivity<sup>12</sup> of 2PPE opens the possibility to probe the linewidth of these states in detail. It is especially well suited for studying states with intrinsic linewidths down to 15 meV like the  $n=1$  image state and additional broadening effects induced, for example, by adsorption. Time-resolved 2PPE is then the superior method for longer-living states. Additional experimental results should lead to a better understanding of the interaction of electrons with surfaces and to a refinement of theoretical models.

This work was supported by the Deutsche Forschungsgemeinschaft (Bonn, Germany).

<sup>1</sup>P. M. Echenique and J. P. Pendry, *J. Phys. C* **11**, 2065 (1978).

<sup>2</sup>P. L. de Andres, P. M. Echenique, and F. Flores, *Phys. Rev. B* **39**, 10356 (1989).

<sup>3</sup>W. Steinmann, *Appl. Phys. A* **49**, 365 (1989), and references therein.

<sup>4</sup>N. V. Smith, *Phys. Rev. B* **32**, 3549 (1985).

<sup>5</sup>S. Schuppler, N. Fischer, W. Steinmann, R. Schneider, and E. Bertel, this issue, *Phys. Rev. B* **42**, 9403 (1990).

<sup>6</sup>G. Borstel, G. Thörner, M. Donath, V. Dose, and A. Goldmann, *Solid State Commun.* **55**, 469 (1985).

<sup>7</sup>P. de Andres, P. M. Echenique, and F. Flores, *Phys. Rev. B* **35**, 4529 (1987).

<sup>8</sup>T. S. Rahman and D. L. Mills, *Phys. Rev. B* **21**, 1432 (1980).

<sup>9</sup>P. M. Echenique, F. Flores, and F. Sols, *Phys. Rev. Lett.* **55**, 2348 (1985).

<sup>10</sup>R. W. Schoenlein, J. G. Fujimoto, G. L. Eesley, and T. W. Capehart, *Phys. Rev. Lett.* **61**, 2596 (1988); *Phys. Rev. B* **41**, 5436 (1990).

<sup>11</sup>H. B. Nielsen, G. Brostroem, and E. Matthias, *Z. Phys. B* **77**, 91 (1989).

<sup>12</sup>S. Schuppler, N. Fischer, Th. Fauster, and W. Steinmann, *Appl. Phys. A* **51**, 322 (1990).

<sup>13</sup>R. Schneider (private communication).

<sup>14</sup>F. J. Himpsel, J. A. Knapp, and D. E. Eastman, *Phys. Rev. B* **19**, 2872 (1979).